Unexpected Broadband Optical Limiting Properties of Antimonene Quantum Dots

Zhiyuan Wang, [a] Chenxia Hu, [b] Shuai Feng, [a] Zhixin Yao, [a] Peizhi Liu, [a] Hua Wang, [a]* Bingshe Xu, [a] Min Zhao, [a]* Junjie Guo [a]*

[a] Taiyuan University of Technology, Key Laboratory of Interface Science and Engineering in Advanced Materials, Ministry of Education, Research Center of Advanced Materials Science and Technology, Taiyuan, China, 030024
[b] Lanzhou University, State Key Laboratory of Applied Organic Chemistry, College of Chemistry and Chemical Engineering, Key Laboratory of Special Function Materials and Structure Design, Ministry of Education, Lanzhou China, 730000.

Abstract: Antimonene has been found to possess excellent nonlinear refractive and saturable absorption properties recently. To further investigate its optical limiting properties, we prepared uniform antimonene quantum dots (AMQDs) via a facile ionic liquid-assisted exfoliation method. Thereafter the nonlinear absorption of the atomically thin AMQDs was studied using the open aperture Z-scan technique in the nanosecond laser pulse regime. Z-scan measurements indicate that the prepared AMQDs exhibited superior optical limiting properties at 532 nm and 1064 nm excitation, implying the antimonene hold potential for developing broadband nonlinear optical devices.

1   Introduction

Among various nonlinear optical materials, optical limiters have been applied in laser beam shaping and laser damage prevention. [1-4] Up to now, diverse optical limiters have been developed, such as two-dimensional (2D) materials, [5, 6] inorganic carbon-based materials, [7,8] conducting polymers, [9] small organic molecules, [10] and quantum dots. [11-13] Compared with all the other optical limiting materials, 2D materials have received the most attention due to their special structure. [14, 15] Since the discovery of single layer graphene in 2004, the optical limiting properties of graphene and graphene-like 2D materials have been studied comprehensively. [16-21] Significant progress has been made in the development of graphene-like 2D optical limiting materials, such as transition metal dichalcogenides (TMDs, e.g., MoS_2, [19] WS_2, [20]) and black phosphorous (BP) [21]. To further compare the reported 2D optical limiting materials, we find the zero bandgap and weak electronic on/off ratio of graphene limits their use in nonlinear optical applications. [22] The bandgap of 2D TMDs is ranging from 1 to 2.5 eV and the relatively wide

bandgap is not applicable in near-infrared nonlinear optical device [23, 24]. Black phosphorous (BP), possessing a thickness-dependent direct band-gap (0.3-1.5 eV), show promising nonlinear optical properties in both visible and near-infrared region. [25,26] Regrettably, BP is unstable in air and prone to degradation in the atmosphere. [27, 28] What's more, the process of synthesizing single atomic layer BP is complicated. So stable and easily prepared 2D material with wide band-gap similar to black phosphorus is needed.

Fortunately, antimonene (AM) has been recently explored as an interesting 2D layered material similar to BP. [29, 30] The stable few-layer AM can be isolated from the typical semimetal bulk Sb. Theoretical calculations point out that the monolayer AM possesses a bandgap of 1.2-1.3 eV and extraordinary physical properties, such as high carrier mobility and thermal conductivity. [31-33] Up to date, Zhang et al. [34, 35] investigated nonlinear optical response of few-layer AM and AM quantum dots (QDs) at the visible wavelength, and it is shown that AM possesses a giant nonlinear refractive index of $\approx 10^{-5}$ cm^2 W^{-1}. Simultaneously, Zhang et al. [36] studied the saturable absorption properties of few-layer AM. To extend its nonlinear optical properties, the optical limiting properties of the AM are needed to be investigated.

In this work, we prepared high-quality and stable AMQDs with an average size of 2 nm by sonication-assisted exfoliation of Sb powder in 1-ethyl-3-methylimidazolium trifluoroacetate ([EMIM]CF$_3$COO) according to the previous method. Then we investigated optical limiting properties of the prepared AMQDs dispersed in water and N, N-dimethylformamide (DMF) via open aperture Z-scan technique. The results indicate the prepared AMQDs exhibited superior optical limiting properties at 532 nm and 1064 nm excitation in the nanosecond laser pulse regime, facilitating the use of AMQDs in future photoelectric devices.

2   Experimental section

2.1 Preparation of Antimonene Quantum Dots (AMQDs)

AMQDs were prepared according to our previous work method. Briefly, Antimony (Sb) shots (99.999%) were purchased from Aladdin. 1-ethyl-3-methylimidazolium trifluoroacetate ([EMIM]CF_3COO) (≥99%) was purchased from Lanzhou Greenchem ILs, LICP, CAS, China (Lanzhou, China). Appropriate amount of Sb powder was put into a 20 mL vial with 10 mL of [EMIM]CF_3COO, and continuously sonicated for 10 h in ice bath at 500 W delivering the ultrasound power in pulses 1 s long every 2 s (GUIGO-92-IIDN ultrasonic processor equipped with a 6 mm sonotrode, China). The resulting dispersion was centrifuged and washed.

2.2 Characterizations

Transmission electron microscopy (TEM, JEM-2100F, JEOL, Japan) and atomic-force microscopy (AFM, SPA-300HV, Japan) were applied to characterize the morphology of the AMQSs. X-ray diffraction (XRD, D8 Discover, Germany) were used to analyze the crystal structure of AMQSs. Raman spectra were recorded using a Renishaw in via Raman Microscope System with an excitation wavelength of 514 nm. UV/vis absorption spectra were obtained using UV/vis spectrophotometer (HITACHI U-3900).

2.3 Z-scan setup.

The nonlinear optical response of AMQSs is further investigated at 532 nm and 1064 nm via open aperture Z-scan technique according to the previous work. [13] Briefly, 4 ns (FWHM), 532 nm and 1064 nm laser pulses with a repetition rate of 10 Hz from a Q-switched Nd:YAG laser (Continuum, Model Surelite SL-I-10) were used as the light source. Two corresponding pyroelectric detectors (Laser Probe, RJ-735; with RJ7620 dual channel power meter) were used

to measure changes in laser transmission. The samples were placed in quartz cells with a thickness of 2 mm.

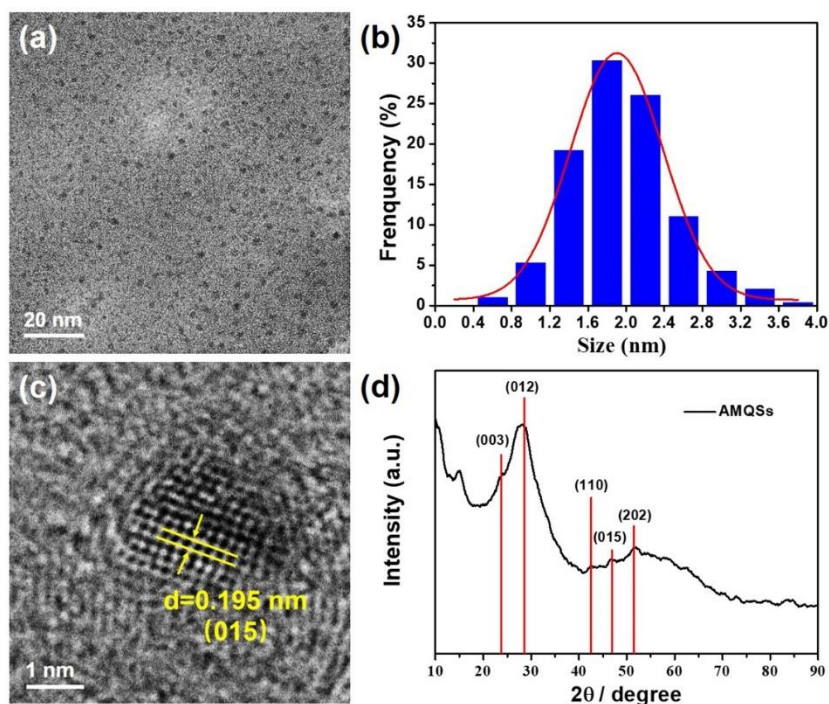## 3   Results and discussion

Fig. 1 Structural characteristics of AMQDs: (a) TEM and (d) HRTEM images of the AMQDs. (b) Statistical histogram of diameter distribution of 280 samples corresponding to (a). (d) Wide-angle XRD patterns of the AMQDs.

AMQDs were prepared via ion-intercalation and sonication-assisted exfoliation of Sb powder in [EMIM]CF$_3$COO. After a complete exfoliation, AMQDs were characterized by Transmission electron microscopy (TEM). As shown in Figure 1a, the AMQDs possess uniform size and good dispersibility, which suggest that high-quality AMQDs has been obtained in this way. As shown in Figure 1b, over 280 samples were measured to get the diameter distribution of AMQSs and the result indicates that the average size of the product is ~2 nm. Figure 1c exhibits the high-resolution TEM (HRTEM) of a single AMQD and the lattice distance is ~0.195 nm, which can

be corresponded to (015) lattice plane. Furthermore, the crystal structure of AMQDs was further confirmed by X-ray diffraction (XRD) spectrum. As shown in Figure 1d, the diffraction patterns of AMQDs can be assigned to (003), (012), (110), (015) and (202) lattice planes of hexagonal Sb (JCPDS NO. 350732). But the peaks of AMQDs are dramatically weakened compared to bulk Sb, since the graphene-like nanosheets lack long-range atomic order in the third dimension. [37]
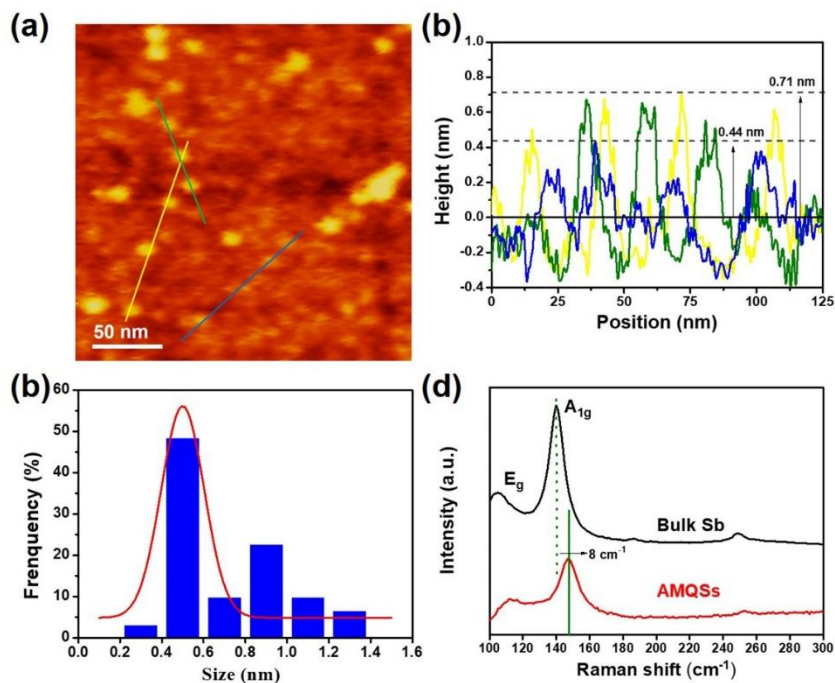

Fig. 2 Morphological characterizations of AMQDs: (a) AFM image of the AMQDs. (b) Height analysis of typical samples. (c) Statistical histogram of the thicknesses distribution of 30 samples corresponding to (a). (d) Raman spectra of the as-prepared AMQDs and its bulk counterpart.

The height of the sample was characterized by atomic force microscopy (AFM). Figure 2a is the AFM image of AMQDs, height and thickness analysis of more than 30 selected AMQD samples is shown in Figure 2b and Figure 2c. The result show that the average thickness of AMQDs is 0.7 nm, and more than 54% of the AMQDs have thicknesses in the range of 0.4~0.6 nm, i.e. around monolayer. [29] In order to further investigate the structure and quality of AMQDs, Raman spectroscopy was carried out and Figure 2d presents the Raman spectra of bulk Sb and
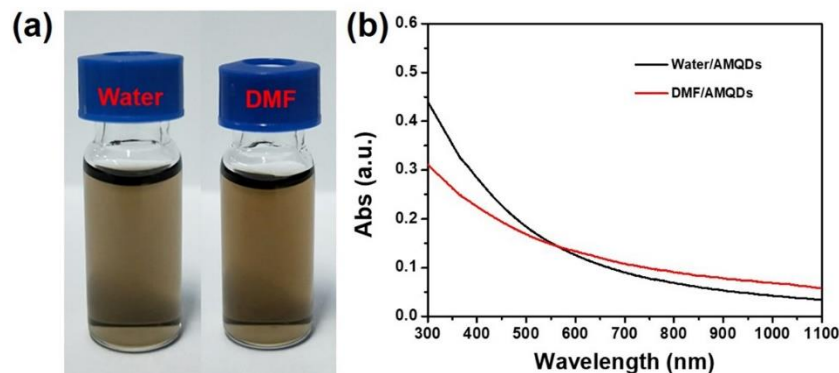
Fig. 3 Characterizations of AMQDs of linear spectral absorption: (a) Photographs of the AMQSs dispersed in water and DMF. (b) UV-vis absorption spectra of AMQSs dispersed in water and DMF.

AMQDs excited by the 514 nm laser. All the samples show two modes of resonance peaks, A_{1g} mode peak and E_g mode peak. Bulk Sb crystal owns A_{1g} mode peak at 139.8 cm^{-1} and E_g mode peak at 105.1 cm^{-1} originating from the microcrystalline. After exfoliation, the AMQDs show different A_{1g} mode peak at 147.2 cm^{-1} and E_g mode peak at 112.5 cm^{-1}, indicating the successful preparation of antimonene. Figure 3a is the photograph of our prepared AMQDs dispersed in water and DMF, which shows that the products have excellent dispersion in these two solvents. Figure 3b is the ultraviolet-visible (UV-vis) absorption spectra for AMQDs respectively, showing broadband absorption of AMQDs.

In order to investigate the nonlinear optical absorption of AMQDs, a typical open aperture Z-scan measurement was carried out via the method of the reported literature. [13, 37] Briefly, open aperture (OA) Z-scan experiments were performed at 532 and 1064 nm. The linear transmittances of all the samples were adjusted to be T = 75% at 532 nm and 85% at 1064 nm with pulse width of 4 ns (FWHM). The input laser pulse energy was 4.3 µJ, 15 µJ and 42 µJ at 532 nm and 44 µJ, 150 µJ and 220 µJ at 1064 nm, respectively. In this measurement, normalized transmittance of 1.0 indicates that the material plays no nonlinear absorption behavior. When the

normalized transmittance above 1.0, the sample exhibits saturable absorption. In contrast, the sample exhibits reverse saturable absorption.
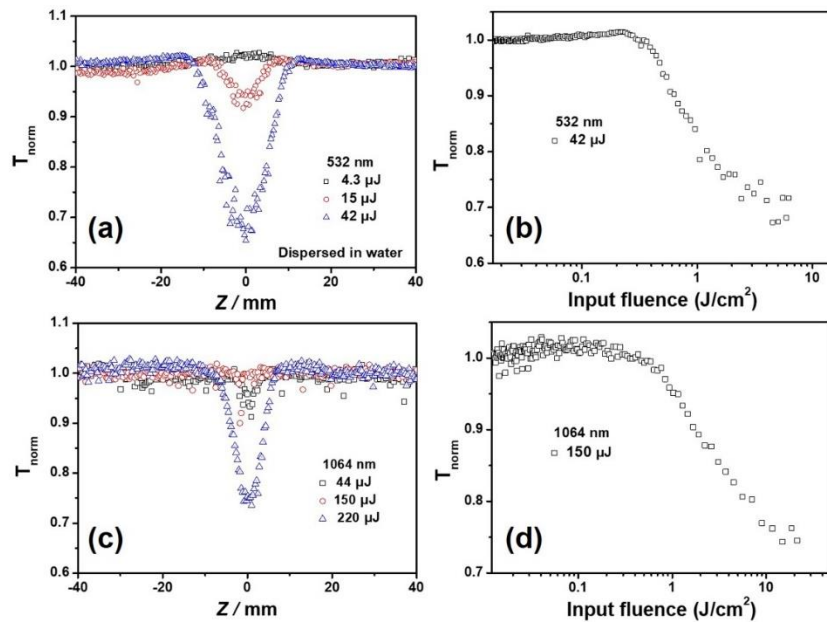

Fig. 4 The open-aperture Z-scan measurements of the as prepared AMQDs dispersed in water: Open-aperture Z-scan curves of AMQDs dispersions and a linear transmittance of 75% at 532 nm (a) and a linear transmittance of 85% at 1064 nm (c). (b) and (d) The plots of transmittance versus input fluence corresponding to (a) and (c), respectively.

Figure 4a shows the open aperture Z-scan data of AMQDs dispersed in water with different input laser energy at 532 nm. The results show that the sample exhibits weak nonlinear optical absorption at low input laser pulse (4.3 µJ). But when the input laser pulse was 15 µJ, the AMQDs exhibits stronger optical limiting properties. Along with the increase of incident pulse energy (42 µJ), the transmittance is significantly reduced, indicating the stronger optical limiting performance. Similarly, when the input laser pulse energy was more than 220µJ, the AMQDs also present good optical limiting effects at 1064 nm. In addition, a plot of normalized transmittance versus input influence is presented in Fig. 4b and Fig. 4d for AMQDs with input laser pulse energy of 42 µJ at 532 nm and 220µJ at 1064 nm. The optical limiting onset fluence (F_{on}), defined as fluence where transmittance starts to fall to 95% of its original value can be

extracted, [5] is about 0.48 J cm^{-2} at 532 nm and 1.04 J cm^{-2} at 1064 nm. Furthermore, we also

studied the nonlinear optical absorption of AMQDs dispersed in DMF. As shown in Figure 5a

and 5c, the AMQDs show strong optical limiting performance both at 532 nm and 1064 nm as

the input laser energy increases. The F_{on} values is about 0.11 J cm^{-2} with input laser pulse energy

of 42 µJ at 532 nm (Figure 5b) and 1.13 J cm^{-2} with input laser pulse energy of 220µJ at 1064

nm (Figure 5d). In our study, the mechanism of the optical limiting properties of the AMQDs

system is expected to be a result of the combination of nonlinear scattering [8, 38] and free carrier

absorption. [39, 40] This clearly indicates the such strong optical limiting performance of AMQDs

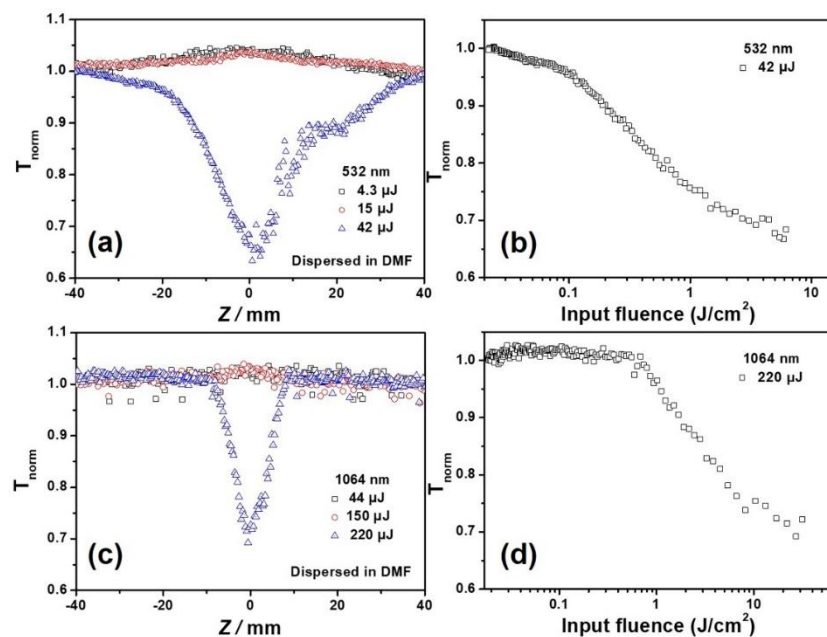in different media implies their potential for developing broadband optical limiting devices.

Fig. 5 The open-aperture Z-scan measurements of the as prepared AMQDs dispersed in DMF: Open-aperture Z-scan

curves of AMQDs dispersions and a linear transmittance of 75% at 532 nm (a) and a linear transmittance of 85% at

1064 nm (c). (b) and (d) The plots of transmittance versus input fluence corresponding to (a) and (c), respectively.

4   Conclusion

In summary, we have synthesized high-quality AMQDs through sonication-assisted exfoliation of Sb powder. Additionally, we thoroughly investigated the nonlinear optical properties of AMQDs via open aperture Z-scan technique and found that the prepared AMQDs exhibit broadband optical limiting response from visible to near-infrared wavelengths. The mechanism of such optical limiting performance is expected to arise from a combination of free carrier absorption and nonlinear scattering. This property makes the new antimonene a good candidate for use in broadband nonlinear optical and optoelectronic devices.

Conflicts of interest

There are no conflicts to declare.

Acknowledgments

References

1. J. Balapanuru, J. Yang, S. Xiao, Q. Bao, M. Jahan, et al., "Graphene oxide-organic dye ionic complex with DNA-sensing and optical-limiting properties," Angew. Chem. Int. Ed., **49**(37), 6549-53 (2010).

2. G. Zhou and W. Wong, "Organometallic acetylides of PtII, AuI and HgII as new generation optical power limiting materials," *Chem. Soc. Rev.*, **40**, 2541-2566 (2011).

3. J. Perry, K. Mansour, Y. Lee, L. Wu, P. Bedworth, et al., "Organic optical limiter with a strong nonlinear absorptive response," *Science,* **273**, 1533-1536 (1996).

4. G. Lim, Z. Chen, J. Clark, R. Goh, W. Ng, et al., "Giant broadband nonlinear optical absorption response in dispersed graphene single sheets," *Nat. Photonics*, **5**, 554 (2011).

5. X. Liu, Q. Guo and J. Qiu, "Emerging low-dimensional materials for nonlinear optics and ultrafast photonics," *Adv. Mater.*, **29**, 1605886 (2017).

6. S. Yu, X. Wu, Y. Wang, X. Guo and L. Tong, "2D materials for optical modulation: challenges and opportunities," *Adv. Mater.*, **29**, 1606128 (2017).

7. H. Wu, D. Liu, H. Zhang, C. Wei, B. Zeng, et al., "Solvothermal synthesis and optical limiting properties of carbon nanotube-based hybrids containing ternary chalcogenides," *Carbon*, **50**(14), 4847 (2012).

8. B. Anand, R. Podila, P. Ayala, L. Oliveira, R. Philip, et al., "Nonlinear optical properties of boron doped single-walled carbon nanotubes," *Nanoscale,* **5**, 7271 (2013).

9. Y. Zeng, C. Wang, F. Zhao, M. Qin, Y. Zhou, et al., "Two-photon induced excited-state absorption and optical limiting properties in a chiral polymer," *Appl. Phys. Lett.*, **102**, 043308 (2013).

10. H. Lei, H. Wang, Z. Wei, X. Tang, L. Wu, et al., "Photophysical properties and TPA optical limiting of two new organic compounds," *Chem. Phys. Lett.*, **333**, 387 (2001).

11. D. Asunskis, I. Bolotin and L. Hanley, "Nonlinear optical properties of PbS nanocrystals grown in polymer solutions," *J. Phys. Chem. C*, **112**, 9555 (2008).

12. T. Wang, B. Gao, Q. Wang, M. Zhao, K. Kang, et al., "A facile phosphine-free method for synthesizing PbSe nanocrystals with strong optical limiting effects," *Chem. - Asian J.*, **8**, 912 (2013).

13. M. Zhao, R. Peng, Q. Zheng, Q, Wang, M. Chang, et al., "Broadband optical limiting response of a graphene-PbS nanohybrid," *Nanoscale*, **7**, 9268-9274 (2015).

14. K. S. Novoselov, A. K. Geim, S. V. Morozov, D. Jiang, Y. Zhang, et al., "Electric field effect in atomically thin carbon films," *Science*, **306**, 666 (2004).

15. K. S. Novoselov, V. I. Falko, L. Colombo, P. R. Gellert, M. G. Schwab, et al., "A roadmap for graphene," *Nature*, **490**, 192 (2012)

16. J. Wang, Y. Hernandez, M. Lotya, J. N. Coleman and W. J. Blau, "Broadband nonlinear optical response of graphene dispersions," *Adv. Mater.* **21**, 2430 (2009).

17. Y. Xu, Z. Liu, X. Zhang, Y. Wang, J. Tian, et al., "A graphene hybrid material covalently functionalized with porphyrin: synthesis and optical limiting property," *Adv. Mater.*, **21**, 1275 (2009).

18. D. Tan, X. Liu, Y. Dai, G. Ma, M. Meunier, et al., "A universal photochemical approach to ultra-small, well-dispersed nanoparticle/reduced graphene oxide hybrids with enhanced nonlinear optical properties," *Adv. Opt. Mater.,* **3**, 836 (2015).

19. K. Wang, Y. Feng, C. Chang, J. Zhan, C. Wang, et al., "Broadband ultrafast nonlinear absorption and nonlinear refraction of layered molybdenum dichalcogenide semiconductors," *Nanoscale,* **6**(18), 10530-10535 (2014).

20. S. Zhang, N. Dong, N. Mcevoy, M. O'Brien, S. Winters, et al., "Direct observation of degenerate two-photon absorption and its saturation in WS_2 and MoS_2 monolayer and few-layer films," *ACS Nano,* **9**(7), 7142-7150 (2015).

21. X. Jiang, Z. Zeng, S. Li, Z. Guo, H. Zhang, et al., "Tunable broadband nonlinear optical properties of black phosphorus quantum dots for femtosecond laser pulses," *Materials,* **10**, 210 (2017).

22. M. Naguib, M. Kurtoglu, V. Presser, J. Lu, J. Niu, et al., "Two-dimensional nanocrystals produced by exfoliation of Ti_3AlC," *Adv. Mater.*, **23**, 4248 (2011).

23. K. F. Mak, C. Lee, J. Hone, J. Shana and T. F. Heinz, "Atomically thin MoS_2: a new direct-gap semiconductor," *Phys. Rev. Lett.*, **105**, 136805 (2010).

24. A. Splendiani, L. Sun, Y. B. Zhang, T. Li, J. Kim, et al., "Emerging photoluminescence in monolayer MoS_2," *Nano Lett.*, **10**, 1271 (2010).

25. Y. Du, C. Ouyang, S. Shi and M. Lei, "Ab initio studies on atomic and electronic structures of black phosphorus," *J. Appl. Polym. Sci.*, **107**(33), 093718 (2010).

26. O. Prytz and E. Flage-Larsen, "The influence of exact exchange corrections in van der Waals layered narrow bandgap black phosphorus," *J. Phys.: Condens. Matter*, **22**, 015502 (2010).

27. M. T. Edmonds, A. Tadich, A. Carvalho, A. Ziletti, K. M. O'Donnell, et al., "Creating a stable oxide at the surface of black phosphorus," *ACS Appl. Mater. Interfaces*, **7**, 14557 (2015).

28. T. Zhang, Y. Wan, H. Xie, Y. Mu, P. Du, et al., "Degradation chemistry and stabilization of exfoliated few-layer black phosphorus in water," *J. Am. Chem. Soc.,* **140**, 7561-7567 (2018).

29. P. Ares, F. Aguilar-Galindo, D. Rodriguez-San-Miguel, D. A. Aldave, S. Diaz-Tendero, et al., "Mechanical isolation of highly stable antimonene under ambient conditions," *Adv. mater.*, **28**, 6332 (2016).

30. J. Ji, X. Song, J. Liu, Z. Yan, C. Huo, et al., "Two-dimensional antimonene single crystals grown by van der Waals epitaxy," *Nat. Commun.*, **7**, 13352 (2016).

31. S. Zhang, Z. Yan, Y. Li, Z. Chen and H. Zeng, "Atomically thin arsenene and antimonene: semimetal-semiconductor and indirect-direct band-gap transitions," *Angew. Chem. Int. Ed.*, **54**, 3112 (2015).

32. S. Zhang, M. Xie, F. Li, Z. Yan, Y. Li, et al., "Semiconducting group 15 monolayers: a broad range of band gaps and high carrier mobilities," *Angew. Chem. Int. Ed.*, **55**, 1666 (2016).

33. Y. Wang and Y. Ding, "The electronic structures of group-V-group-IV hetero-bilayer structures: a first-principles study," *Phys. Chem. Chem. Phys.*, **17**, 27769 (2015).

34. L. Lu, X. Tang, R. Cao, L. Wu and Z. Li, "Broadband nonlinear optical response in few-layer antimonene and antimonene quantum dots: a promising optical kerr media with enhanced stability," *Adv. Optical Mater.*, **5**(17), 1700301 (2017).

35. Y. Song, Y. Chen, X. Jiang, W. Liang, K. Wang, et al., "Nonlinear few-layer antimonene-based all-optical signal processing: ultrafast optical switching and high-speed wavelength conversion," *Adv. Optical Mater.*, **6**(13), 1701287 (2018).

36. Y. Song, Z. Liang, X. Jiang, Y. Chen, Z. Li, et al., "Few-layer antimonene decorated microfiber: ultra-short pulse generation and all-optical thresholding with enhanced long term stability," *2D Materials*, **4**(4), 045010 (2017).

37. M. Zhao, K. Liu, Y. Zhang, Q. Wang, Z. Li, et al., "Singlet fission induced giant optical limiting responses of pentacene derivatives," *Mater. Horiz.*, **2**, 619-624 (2015).

38. M. Feng, H. Zhan and Y. Chen, "Nonlinear optical and optical limiting properties of graphene families," *Appl. Phys. Lett.,* **96**, 033107 (2010).

39. L. Tutt and T. Boggess, "A review of optical limiting mechanisms and devices using organics, fullerenes, semiconductors and other materials," *Prog. Quantum Electron.,* **17**, 299-338 (1993).

40. R. Philip, P. Chantharasupawong, H. Qian, R. Jin and J. Thomas, "Evolution of nonlinear optical properties: from gold atomic clusters to plasmonic nanocrystals," *Nano Lett.,* **12**, 4661 (2012).